Modelling the effects of resin shrinkage in pultrusion of composites sections

Joshi, Sunil C.

2000

Lam Y. C., & Joshi, S. C. (2000). Modelling the effects of resin shrinkage in pultrusion of composites sections. Advanced Composites Letters, 9(6).

https://hdl.handle.net/10356/80855

MODELLING THE EFFECTS OF RESIN SHRINKAGE IN PULTRUSION OF COMPOSITES SECTIONS

Sunil C. Joshi* and Y.C. Lam

School of Mechanical & Production Engineering,
Nanyang Technological University, Singapore 639 798.

ABSTRACT

This paper discusses the development, implementation and application of numerical schemes for modelling the effects of temperature-dependent material properties including chemical shrinkage and thermal expansion of resin on the curing of thermosetting composites in pultrusion. The results of the three-dimensional simulation of heat and mass transfer in pultrusion of regular as well as irregular and hollow sections are presented.

KEY WORDS: Pultrusion, Polymer composites, Finite element analysis.

NOMENCLATURE

A	Cross-sectional area	V	Volume
C_p	Specific heat	w	Pull speed
D	Depth	W	Width
k	Thermal conductivity	X,Y,Z	Cartesian axes system
L	Length	α	Degree of cure
m	Mass fraction	ρ	Density
t	Time	ε	Coefficient of thermal expansion
T	Temperature	δ	Small change in unit dimension
v	Volume fraction	γ	Percentage volumetric shrinkage

Operators and descriptors

∇	Differential operator	Δ	Small quantity descriptor
$\frac{d}{dt}$	Rate of change	$[\bar{\ }]$	Tensor notation

*Author for correspondence: mscjoshi@ntu.edu.sg, Fax: (65) 791 1859.

Subscripts

c	Composites	*r*	Resin or matrix
f	Fibre reinforcement	*T*	Total or final quantity
		0	Initial value

Superscripts

j, j-1	Control volumes	*s*	Fully cured resin
		u	Uncured resin

1. INTRODUCTION

Pultrusion is one of the composites manufacturing processes used for continuous fabrication of constant cross-section components. Since mechanical performance of a pultruded part depends upon the quality of its cure, the understanding of heat and mass transfer and resin cure in pultrusion is extremely important.

In the past, many researchers [e.g. 1-7] have used computer simulation to model these phenomena. However none of them considered the effects of temperature-dependent material properties and resin shrinkage in pultrusion of hollow and irregular composites parts.

Thermal properties k and C_p of a fully cured thermosetting resin are usually 30-40% higher than that of the uncured resin [8]. In pultrusion, as resin cures, composites part separates from die wall due to resin shrinkage [2]. This affects the heat transfer between the die and the component, the uniformity of resin cure and the dimensions of the pultruded part. If overlooked, these effects may lead to erroneous results during process simulation.

In the present investigation, numerical schemes for modelling the effects of temperature-dependent material properties including chemical shrinkage and thermal expansion of resin on the curing of thermosetting composites during pultrusion are developed. These schemes were implemented using the three-dimensional Finite Element/ Nodal Control Volume (FE/NCV) simulation procedure developed and published earlier by the authors [7].

A case study on cylindrical rod was carried out based on the published data [3] to validate the developed simulation procedure. The geometry was further used to study the effects of temperature-dependent material properties. An example on bridge deck section with an internal die was included to demonstrate the usefulness and application of the numerical procedure in modelling pultrusion of irregular and hollow composites sections.

2. FE/ NCV MODELLING

The FE/NCV discretization of a pultrusion die with component is shown in Fig. 1. In this modelling approach the movement of resin-saturated composite preform is simulated as a semi-steady process [7]. For each of the control volumes, parameters such as T and α, and material properties such as ρ_c, C_{p_c} and $\bar{k}_c$ are assumed constant over a Δt. The exothermic effects of cure reaction were added as a source term in the heat energy equation; the detailed numerical procedure may be found in [9]. The numerical schemes developed to account for the convective heat transfer and the shrinkage of composites whose properties are functions of control volume temperatures are discussed below.

Convective effects on temperature

To satisfy the principle of energy conservation, the energy in a control volume should be in equilibrium. The energy of a control volume depends upon its original temperature and the thermal energy flowing in or out of it. Thus, when over a Δt, a volume of composite, ΔV^j, moves from control volume $j-1$ to control volume j (Fig. 1) and the same amount of composites leaves j, the energy balance may be written as:

$$\rho_c^j C_{pc}^j V^j T^j + \Delta V^j \left[(\rho_c^{j-1} C_{pc}^{j-1} T^{j-1}) - (\rho_c^j C_{pc}^j T^j) \right] = \rho_c^j C_{pc}^j V^j (T^j + \Delta T^j) \qquad (1)$$

where, $\Delta V^j = wA^j \Delta t$ and $V^j = L^j A^j$.

For the case of hexahedron control volumes, as shown in Fig. 1, $A^j = W^j D^j$. With these conventions, Eq. (1) can be further simplified to obtain ΔT^j as:

$$\Delta T^j = \lambda^j (\psi^j T^{j-1} - T^j) \tag{2}$$

where, $\lambda^j = \frac{\Delta V^j}{V^j} = \frac{w\Delta t}{L^j}$, and $\psi^j = \frac{\rho_c^{j-1} C_{pc}^{j-1}}{\rho_c^j C_{pc}^j}$.

The ΔT^j is then added to T^j to obtain the current temperature T_T^j.

Convective effects on resin cure

When a composite mass either leaves or enters a control volume, state of cure of the control volume changes in the same proportion as that of the mass. Such a change in α for control volume j, $\Delta\alpha^j$, can be calculated using a volume-average technique as:

$$\Delta\alpha^j = \frac{\Delta V^j}{V^j}(\alpha^{j-1} - \alpha^j) = \lambda^j (\alpha^{j-1} - \alpha^j) \tag{3}$$

The sum of $\Delta\alpha^j$ and α^j gives the final degree of cure, α_T^j.

Dimensional changes

Thermal expansion of resin depends on its temperature. Resin shrinkage is a function of the degree of cure. Therefore, the change in a unit dimension of resin-filled control volume j, δ_r^j, may be calculated as:

$$\delta_r^j = \left[1 + \varepsilon_r (T_T^j - T_0^j)\right] \times \left(1 - \frac{\gamma_r \alpha_T^j}{100}\right)^{\frac{1}{3}} \tag{4}$$

It may be observed from Eq. (4) that the dimensions of a composite part change continuously as its cures in the die. In the present approach, it is assumed that such changes occur only in the cross-sectional (i.e. X and Y) dimensions of a pultrudate. This assumption is valid because the continuous fibre reinforcement and the applied pulling force overshadow the

dimensional changes due to thermal expansion and shrinkage of resin in the longitudinal (Z) direction.

After each time step, the X and Y dimensions of control volume j are calculated by multiplying its original dimensions by factor δ_c^j, which is calculated from δ_r^j, assuming that only the matrix contributes to the dimensional changes, as:

$$\delta_c^j = v_r \delta_r^j + v_f = 1 - v_r (1 - \delta_r^j) \tag{5}$$

It is also assumed that the axis of gravity (i.e. the Z-axis) of the component acts as a zero-shrinkage axis and all the dimensional changes in the component take place with reference to this axis. During simulation, X and Y coordinates of the zero-shrinkage axis are supplied as input data to the program. The new coordinates of a node are then obtained by summing the new X and Y dimensions of all the control volumes that lie on the line connecting the axis of gravity to that particular node.

Thus, at the end of every time step the changes in the all cross-sections of the component that lie within the forming die are calculated. The updated nodal coordinates are then used to drive the subsequent step of the analysis.

It may be noted that some of the component edges, especially for the case of hollow sections, cannot shrink freely due to the internal dies. Before starting the analysis such edges of the component and the degrees of freedom to be restricted are identified; the corresponding boundary conditions are given as input to the program so that the original position of these edges is maintained throughout the analysis.

Changes in the material properties

Ignoring the effects of thermal expansion and chemical shrinkage of resin in the longitudinal direction and using a rule of mixture based on the volume fractions of fibre and matrix, the density of control volume j is calculated at the end of every time step as:

$$\rho_c^j = v_r \left[\rho_r / (\delta_r^j)^2 \right] + v_f \rho_f \tag{6}$$

Similarly, the properties C_p and $\bar{k}$ of the composites contained in control volume j are calculated, using rules of mixture based on m and the final α, as:

$$C_{pc}^j = m_r \left[(1-\alpha_T^j) C_{pr}^u + \alpha_T^j C_{pr}^s \right] + m_f C_{pf} \tag{7}$$

$$\frac{1}{\bar{k}_c^j} = \frac{m_f}{\bar{k}_f} + \frac{m_r}{\left[(1-\alpha_T^j) k_r^u + \alpha_T^j k_r^s \right]} \tag{8}$$

where, $m_f = v_f (\frac{\rho_f}{\rho_c})$ and $m_r = 1 - m_f$.

Heat transfer at die-component interface

In the present approach, the heat transfer between component and die is modelled using the concept of thermal surface [10]. The thermal surfaces are defined along the interface between the peripheral surfaces of the die and the component. Whenever and wherever the thermal surfaces are in direct contact with each other, heat transfer between them takes place only by conduction; the conductance may be defined as a function of the contact pressure. However, as the curing of the component progresses, its dimensions change, which sometimes result in a gap between the thermal surfaces. The new locations of FE nodes on the periphery of the component define the gap. If the gap is narrow, thermal link finite elements are set up between the corresponding FE nodes to affect the heat transfer by conduction and/or convection. The thermal conductivity and the coefficient of convective heat transfer for a thermal link can be defined as a function of the length of the link element. When the gap exceeds the prescribed length, no heat flow is permitted between the surfaces. Thus, the present approach can cater for any localized variations in the gap size. This is necessary when the cross-section of a component is irregular and hollow, and uneven dimensional changes and heat transfer across the die-component interface are expected.

3. NUMERICAL IMPLEMENTATION

A flow chart depicting the solution sequence for the developed FE/NCV procedure is shown in Fig. 2. General-purpose FE package LUSAS [10] is employed to create initial FE models, to perform field analysis and to post-process the results. The user-programs are composed in FORTRAN 77 to supplement the simulation using the above-mentioned and a few other numerical schemes. The FE module and the user-written codes were interfaced using batch files for PC-DOS environment.

It may be noted that T and α for all the control volumes slowly stabilize after the die reaches the maximum set-temperatures in different zones. The simulation may be terminated any time after the output of program UP2 indicates that all the control volumes have satisfied the convergence criteria for T and α. Otherwise, the whole numerical procedure should be repeated over the next time step.

4. CASE STUDIES

The developed simulation procedure was used for studying pultrusion of a cylindrical rod and a bridge deck section.

Cylindrical rod

This example was based on the work of Valliappan et al. [3] and selected primarily to validate the present numerical procedure. The same cylindrical rod geometry (as shown Fig. 3), die temperature profile (as shown in Fig. 4a), materials (Hercules AS4-12K carbon fibre reinforcement with 37.8% of SHELL EPON9420/9470/537 epoxy resin system by volume), material properties and cure kinetics data as contained in [3] were used in the present analysis. The properties of the materials are listed in Table 1 whereas the cure kinetics model for the resin is presented in Table 2. Since thermal loading was constant along the periphery of the

rod cross-section, only a segment of the rod defined by an angle of 0.5*radians* was modelled. The results of the simulation and its comparison with the published data are given in Fig. 4.

The same example was analyzed further with and without considering the effects of temperature-dependent material properties including resin shrinkage. However, v_r was increased from 0.378 to 0.5 so that the influence of the changing material properties could be examined more effectively. The values of ε_r and γ_r were taken as $0.000045 mm/mm/^{\circ}C$ and 4.0% respectively. The thermal surfaces were assumed to be initially in good contact with each other and heat transfer between the composites and the die was considered to be dominated by conduction. Heat flow, which was considered as a linear function of the gap at the die-component interface, was discontinued after the gap increased beyond 2*mm*. The convergence limits for T and α were $0.005\,℃$ and 0.0005 respectively. The pull-speed was 5*mm/seconds*. The results of the analysis are shown in Fig. 5.

Bridge deck section

The details of the hollow bridge deck section along with the external and the internal (or overhanging) dies are shown in Fig. 6. A heating power of 900*W* was supplied to each of the six heating pads to achieve required temperatures in the die. The internal die was without any heat source. Thermocouple mounted at the centre of the each heating pad was used to control the heater temperature within $\pm 1\,℃$. A square heat sink of $50.8mm \times 50.8mm$ was maintained at $50°C$ between the die cross-sections at $Z = 76.2mm$ and $Z = 176.2mm$. The purpose was to avoid early gelation of resin at the die entrance. A heat loss of $10W/m^2°C$ to the environment $(30°C)$ was assumed for all the non-insulated die surfaces. A total of 1488 hexahedron (HX8) and 48 pentahedron (PN6) elements were used to model the part, and 2880 HX8 and 48 PN6 elements were used to model the die.

Except for the glass fibre reinforcement (60% volume content), all the process parameters and material properties were the same as used for the cylindrical rod. The properties of the fibreglass reinforcement listed in Table 1 were taken from [4]. The results of the simulation with and without considering the effects of resin shrinkage and temperature-dependent properties are presented in Figs. 7 and 8.

5. RESULTS AND DISCUSSIONS

Cylindrical rod

It may be observed from Fig. 4 that the results of the present analysis with v_r=0.378 matched well with the published data [3] indicating that the developed simulation procedure is numerically correct and reliable.

The plots presented in Fig. 5 show the effect due to the changes in material properties with temperature, the resin shrinkage and the separation at die-component interface when v_r=0.5. When these were included in the simulation, the maximum temperature at the centre of the rod dropped to 204℃ from 232℃ when none of the above effects were considered. In addition, at the rear die-end, the diameter of the rod reduced from 9.5*mm* to 9.478*mm* and α dropped from 0.9 to 0.84.

Bridge deck section

The plots of T and α measured at points A and B (their locations are marked in Fig. 6b) as a function of the length of the die are shown in Fig. 7. At point A, the results were significantly affected by the temperature-dependent material properties. The maximum temperature at point A dropped from 192℃ to 169℃ and the final α reduced by 23%. Such high variations were seen only at point A, which lied within the thicker portion of the bridge deck section where the influence of the exothermic heat was higher. On the contrary, the variations were less at point B, as it was located at the interface between the deck section and

the die. The maximum contraction of the cross-sectional dimensions of the bridge deck observed during simulation was 0.013*mm* in the X direction and 0.008*mm* in the Y direction. As a consequence, the final profiles of the degree of cure were different from each other when temperature-dependent and temperature-independent properties were used in the analysis; see Fig. 8 for the contour plots.

This highlights the importance of having a simulation procedure for pultrusion such as the present one that can account for changing material properties and heat transfer characteristics at die-component interface as a function of temperature.

6. CONCLUSIONS

It may be concluded from the results of the case studies that the developed FE /NCV procedure is numerically stable, robust, reliable and can be successfully used for the three-dimensional simulation of pultrusion of solid as well as hollow and irregular composites sections. The various numerical schemes developed to cater for convective heat transfer and temperature-dependent effects including shrinkage and thermal expansion of composites were compatible and well suited for the FE/NCV concept of process modelling. It was observed that the numerical predictions could be inaccurate when the effects of temperature-dependent material properties and the separation between composites and pultrusion die is ignored during simulation.

REFERENCES

1. **Hackett R.M., Zhu S.Z.,** "Two-dimensional finite element model of the pultrusion process", *Journal of Reinforced Plastics and Composites*, **11** (1992), 1322-1351.
2. **Batch G.L., Macosko C.W.,** "Heat transfer and cure in pultrusion: model and experimental verification", *AIChE Journal*, **39**/7, (1993), 1228-1241.
3. **Valliappan M., Roux J.A., Vaughan J.G.** and **Arafat E.S.,** "Die and post-die temperature and cure in Graphite/Epoxy composites", *Composites: Part B*, **27B** (1996), 1-9.
4. **Chachad Y.R., Roux J.A., Vaughan J.G.,** "Thermal model for three-dimensional irregular shaped pultruded fiberglass composites", *Journal of Composites Materials*, **6**/30 (1996), 692-721.
5. **Suratno B.R., Ye L., Mai Y.W.,** "Simulation of temperature and curing profiles in pultruded composite rods", *Composite Science and Technology*, **58** (1998), 191-197.
6. **X.L. Liu, I.G. Crouch, Y.C. Lam**, "Simulation of heat transfer and cure in pultrusion using a general-purpose FE package", *Composite Science and Technology*, **60**/6 (1998), 857-864.
7. **Sunil C. Joshi** and **Y.C. Lam,** "Field Analysis and Modelling of Fibre Reinforced Polymer Composites Manufacturing", presented at VIIIth *International conference on Processing and Fabrication of Advanced Materials*, Singapore, (8-10 September 1999).
8. **Rudd C.D., Long A.C., Kendall K.N., Mangin C.G.E.,** "Liquid Moulding Technologies", ed. I, *Chapter 7: material characterisation*, Woodhead publishing limited, Cambridge, England, (1997), 241-247.
9. **Joshi S.C.,** "Investigations on prepreg moulding, RTM and RFI processes of composites manufacturing", *Ph.D. thesis*, Monash University, Clayton campus, Australia, (1998).
10. **LUSAS** version 13.0, *Theory & User's manuals*, FEA Limited, Surrey, UK.

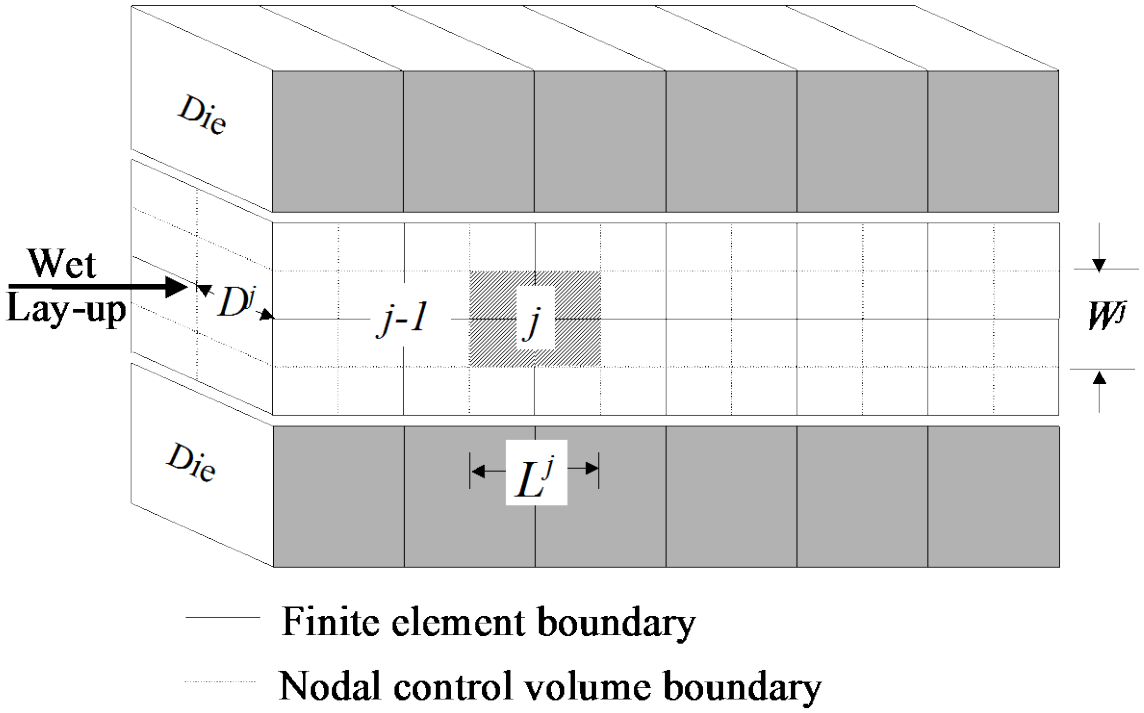

Fig. 1: FE/ NCV model of pultrusion die

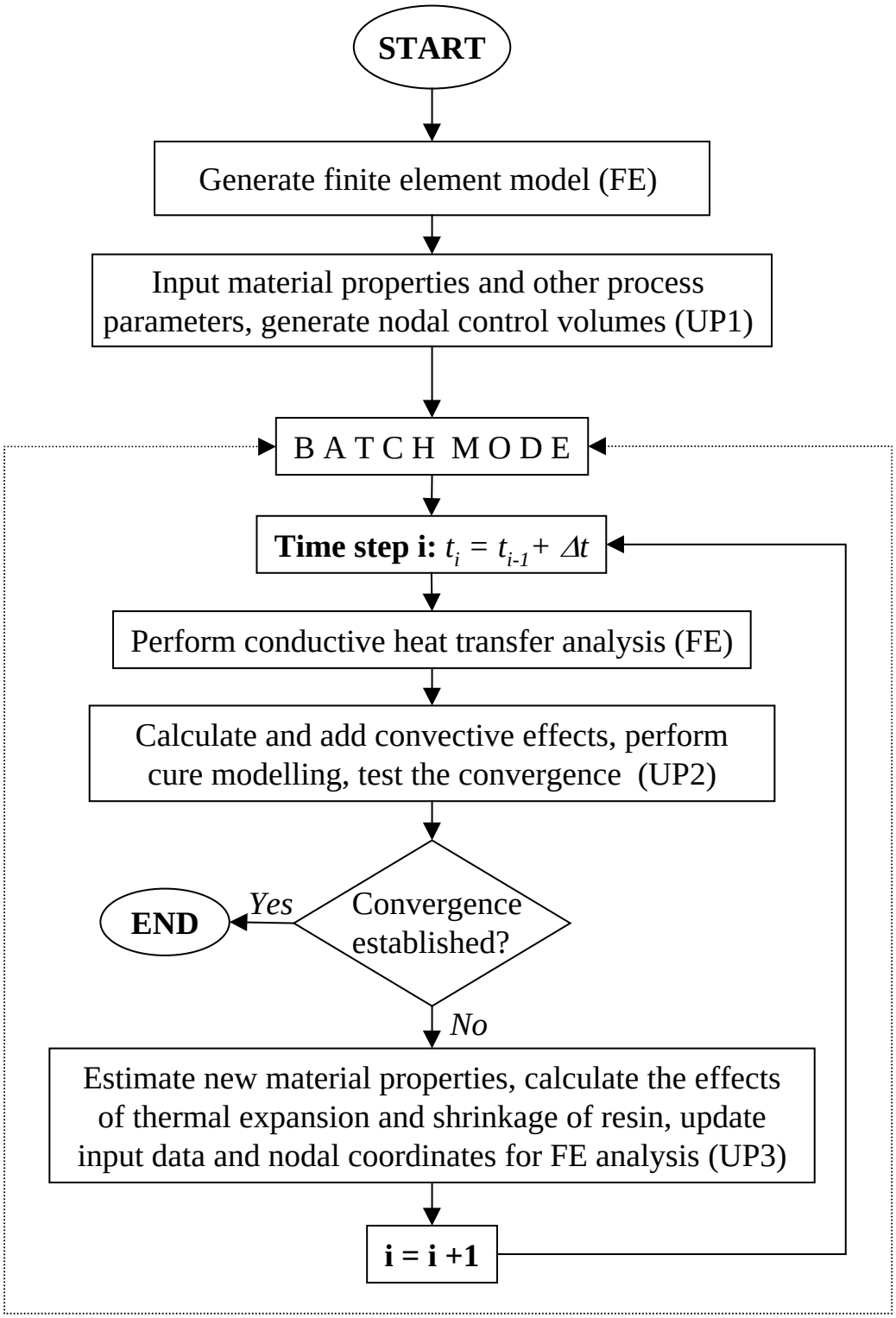

Fig. 2: The proposed FE/NCV simulation procedure for pultrusion (FE: Finite Element package; UP: User-written program)

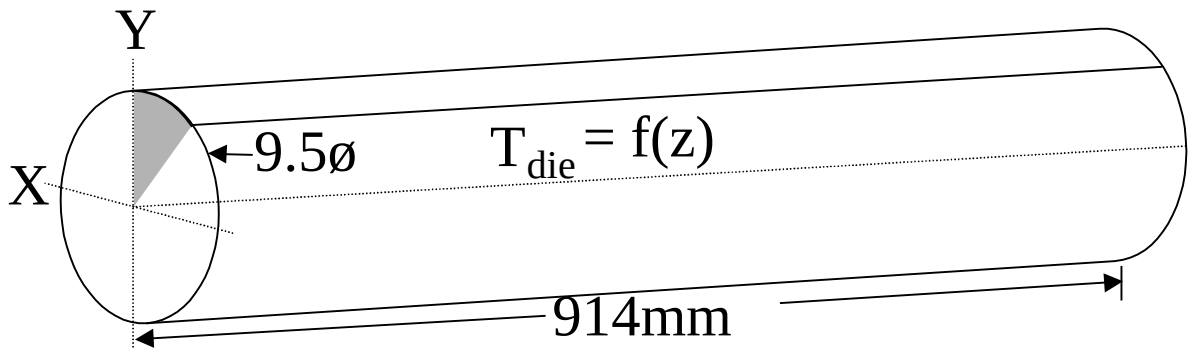

Fig. 3: Details of the cylindrical rod

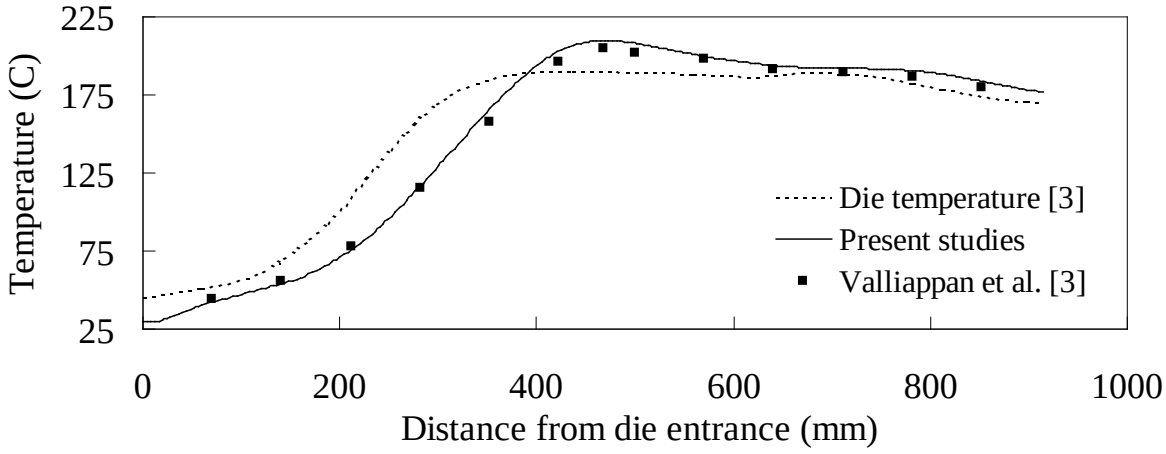

(a)

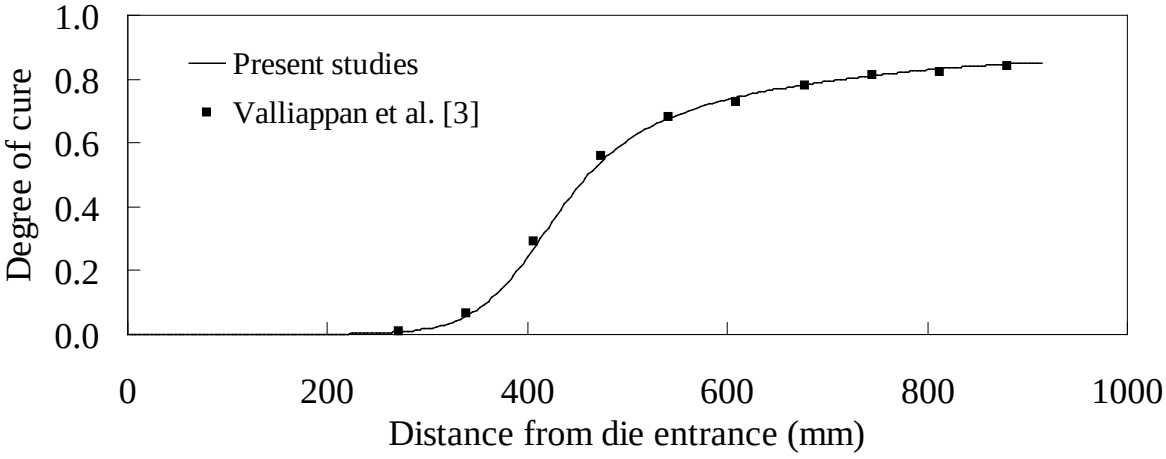

(b)

Fig. 4: Predicted centerline temperature and degree of cure profiles for the cylindrical rod and their comparison with the published data (v_r=0.378)

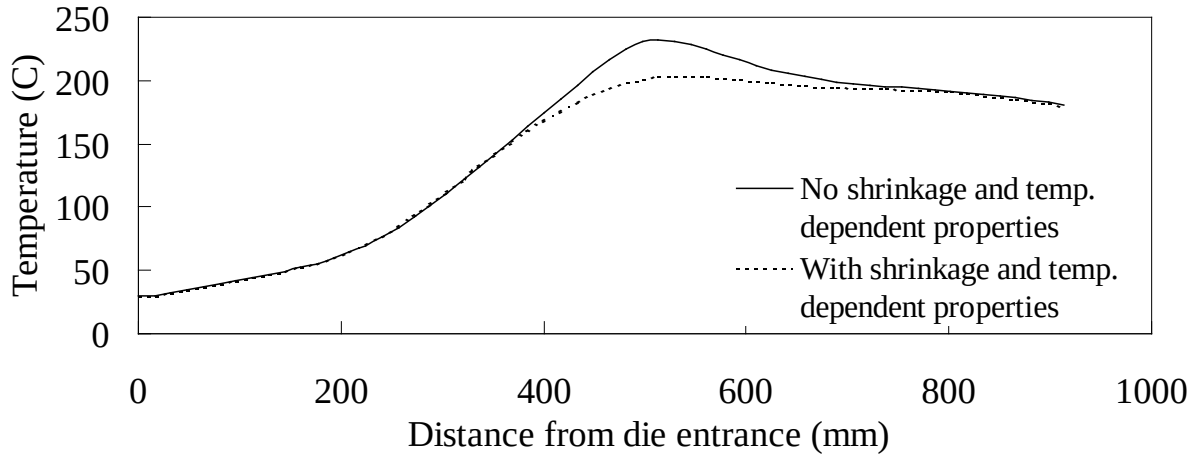

(a)

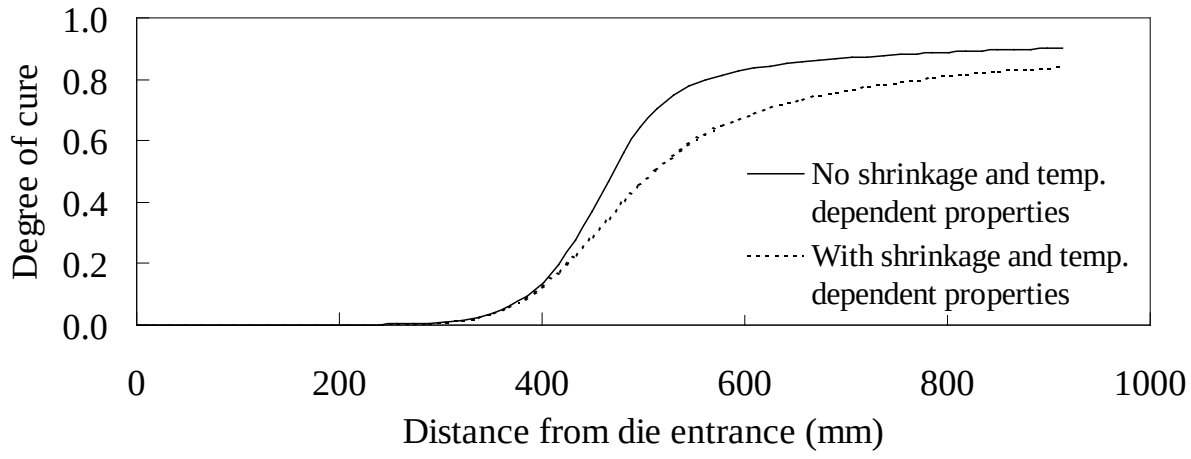

(b)

Fig. 5: Effect of temperature-dependent properties, including chemical shrinkage of resin, on the centreline temperature and degree of cure of the cylindrical rod (v_r=0.5)

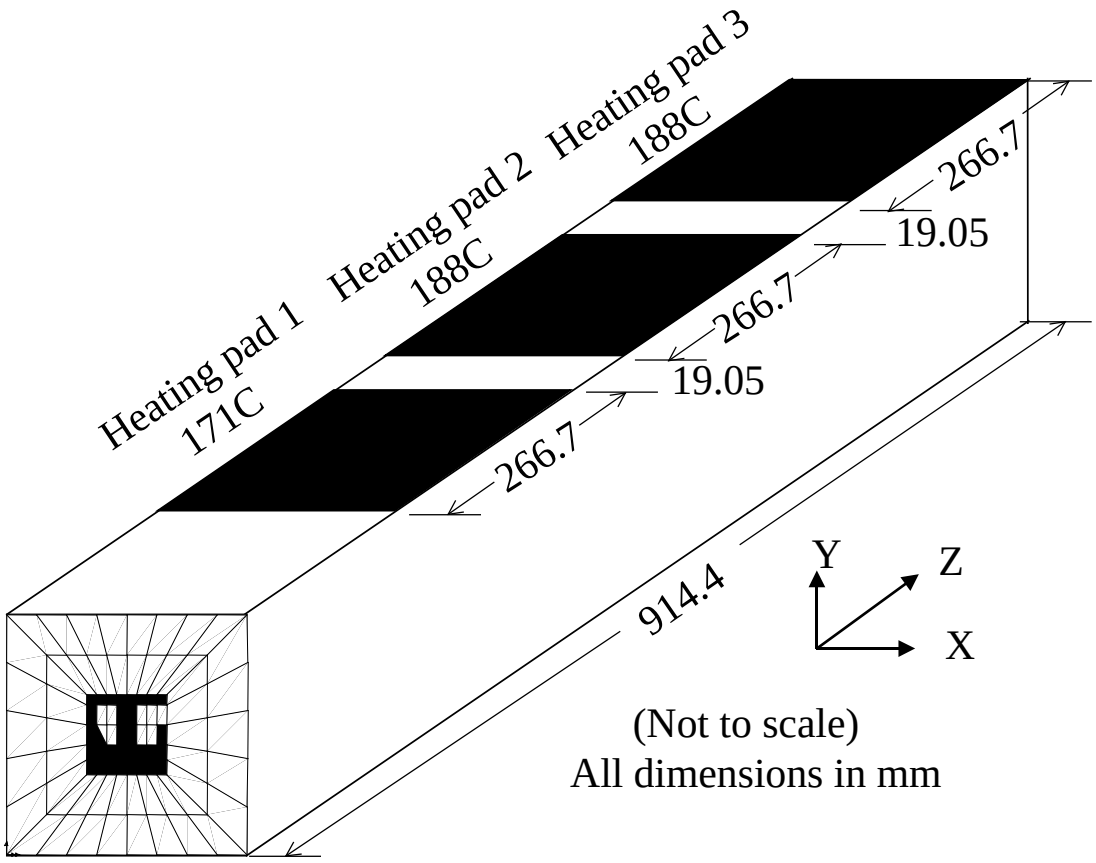

(a) Geometrical details of the die and the heater arrangement

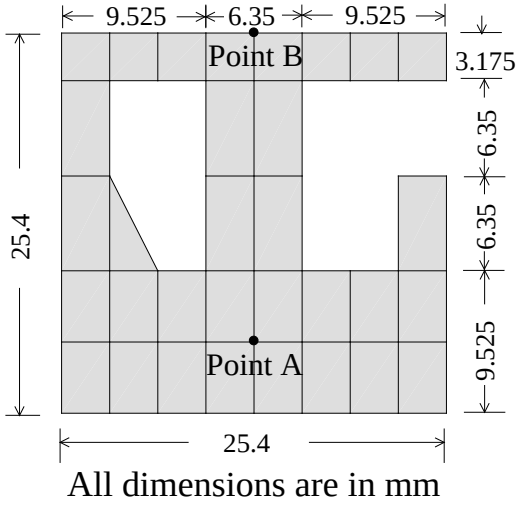

(b) Cross-section of the bridge deck

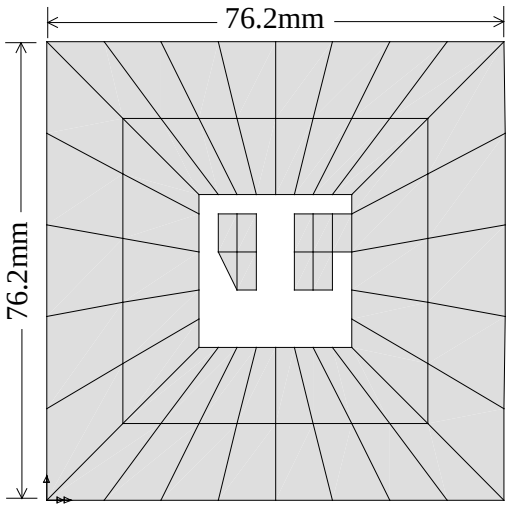

(c) Cross-section of the die

Fig. 6: FE models and other details of the bridge deck section and the die

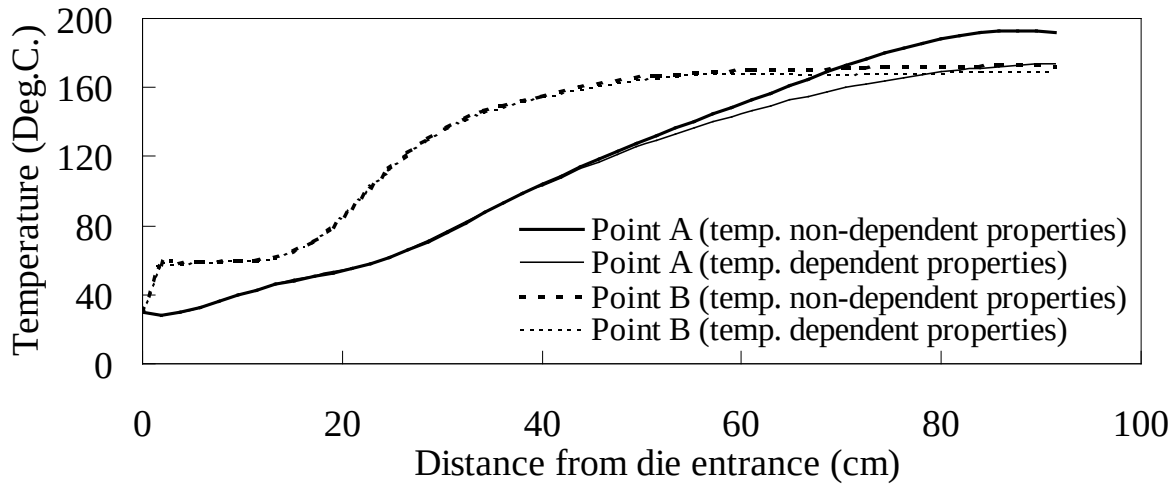

(a)

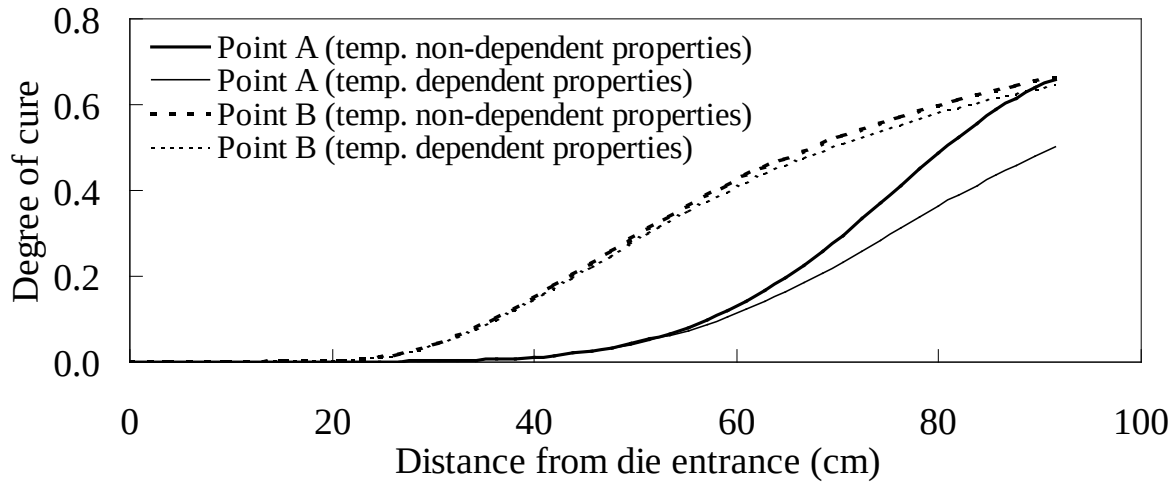

(b)

Fig. 7: Temperature and degree of cure profiles for the bridge deck section

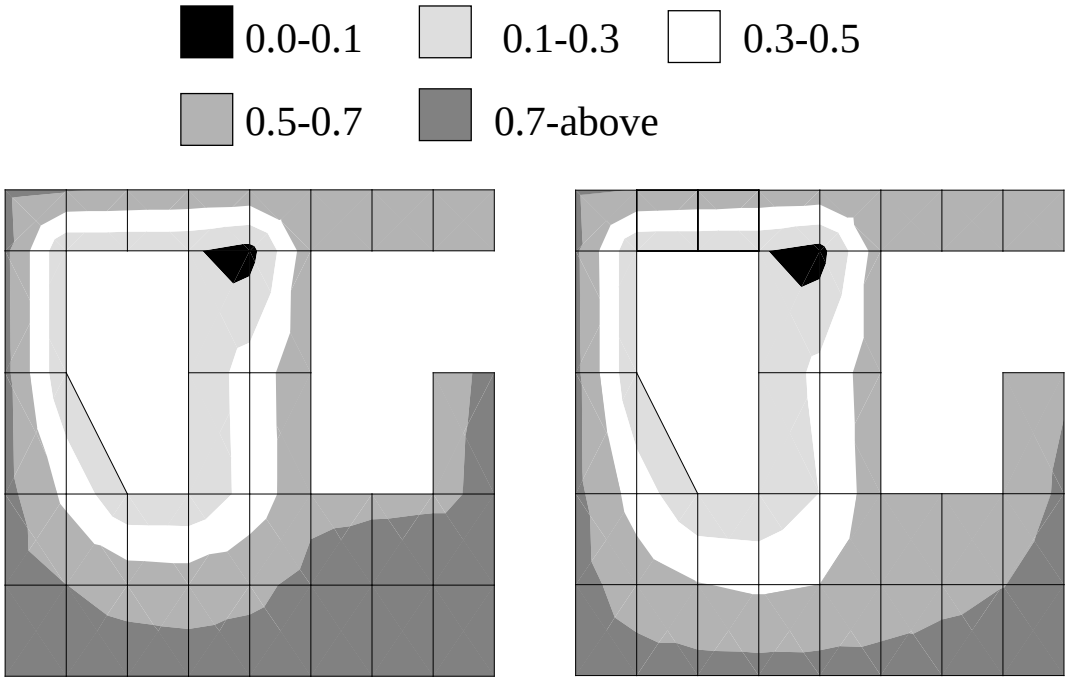

(a) without temperature-dependent material properties

(b) with temperature-dependent material properties

Fig. 8: The final degree-of-cure profiles for the bridge deck section

Table 1: Material properties used for the analysis [3,4]

Material	ρ **(*kg/m*^{3})**	C_p **(*J/kg.K*)**	k **(W/*m.K*)**
Crome steel for die	7833	460	40 [4]
Uncured resin [3]	1260	1255	0.20
Fully cured resin	1260	1568.75$^+$	0.25$^+$
Glass fibres [4]	2560	670	11.4 (longitudinal) 1.04 (cross-fibre)
Carbon fibres [3]	1790	712	66.0 (longitudinal) 11.6 (cross-fibre)

$^+$As learnt from the literature [8], k and C_p of the fully cured resin were assumed to be higher (25%) than the uncured resin.

Table 2: Cure kinetics parameters for EPON 9420/9470/537 epoxy resin system [3]

Arrehenius equation	**Total heat of reaction (*J/gm*)**
$\frac{d\alpha}{dt} = (1.914\times10^{5})e^{(\frac{-6.05\times10^{4}}{RT})}(1-\alpha)^{1.69}$	323.7